Gas-Phase Reaction of Hydroxyl Radical with p-Cymene over an Extended Temperature Range

Yuri Bedjanian,* Julien Morin, Manolis N. Romanias

Institut de Combustion, Aérothermique, Réactivité et Environnement (ICARE), CNRS and Université d'Orléans, 45071 Orléans Cedex 2, France

* To whom correspondence should be addressed. Tel.: +33 238255474, Fax: +33 238696004, e-mail: yuri.bedjanian@cnrs-orleans.fr

ABSTRACT

The kinetics of the reaction of OH radicals with p-cymene has been studied in the temperature range (243 – 898) K using a flow reactor combined with a quadrupole mass spectrometer: OH + p-cymene → products (1). The reaction rate constant was determined as a result of absolute measurements, from OH decay kinetics in excess of p-cymene, and employing the relative rate method with OH reactions with n-pentane, n-heptane,1,3-dioxane, HBr and Br_2 as the reference ones. For the rate coefficient of H-atom abstraction channel the following expression, $k_{1b} = (3.70 \pm 0.42) \times 10^{-11} \exp(-(772 \pm 72)/T)$, was obtained over the temperature range 381 – 898 K. The total rate constant (addition + abstraction) determined at T = (243– 320) K was: $k_1 = (1.82 \pm 0.48) \times 10^{-12} \exp((607 \pm 70)/T)$ or in a biexponential form, $k_1 = k_{1a} + k_{1b} = 3.7 \times 10^{-11} \exp(-772/T) + 6.3 \times 10^{-13} \exp(856/T)$, independent of pressure between 1 and 5 Torr of helium. In addition, our results indicate that the reaction pathway involving alkyl radical elimination upon initial addition of OH to p-cymene is most probably unimportant.

1. INTRODUCTION

The organic compounds emitted from vegetation and plants are classified as Biogenic Volatile Organic Compounds (BVOCs). Global BVOCs emissions are roughly estimated to be 1150 Tg C year^{-1},[1] exceeding by one order of magnitude the emissions of VOCs due to anthropogenic activities.[2-5] The contribution of BVOCs to air quality and climate change is significant since they act as precursor molecules for photochemical smog[6] and secondary organic aerosol formation.[7]

P-cymene ($C_{10}H_{14}$) is an aromatic organic compound representative of BVOCs with a structure consisting of a benzene ring *para*-substituted with methyl and isopropyl groups. It is mainly released from vegetation[8-10] and may also result from atmospheric degradation of some other organic species.[11-12] Upon its emission to the atmosphere, p-cymene is oxidized in reactions with atmospheric detergents (OH, NO_3, O_3, Cl). The understanding of the degradation mechanism of an organic compound in the atmosphere requires information on its major photo-oxidation pathways including kinetics and primary products of its reactions with the atmospheric oxidants. Present study reports an experimental investigation of the reaction of OH radicals with p-cymene, which proceeds through both OH addition and H-atom abstraction channels:

$$OH + C_{10}H_{14}\ (+M) \quad \rightarrow C_{10}H_{14}OH\ (+M) \tag{1a}$$

$$\rightarrow C_{10}H_{13} + H_2O \tag{1b}$$
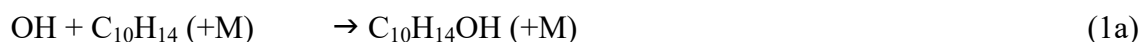
In two previous studies, the measurements of the reaction rate constant with a relative rate method, at room temperature and atmospheric pressure,[13] and absolute measurements, in rather narrow temperature range 299–349 K,[14] were presented. An estimation of the branching ratio of the abstraction channel (1b) at T = 297 K has also been reported.[15] In this work, we report on the measurements of the rate constant of reaction (1) in extended temperature range

T = 243 – 898 K, including temperature dependence of both H-atom abstraction (k_{1b}) and total (k_1) rate constants.

2. EXPERIMENTAL SECTION

Experiments were carried out in a discharge flow tube under laminar flow conditions (Reynolds number < 11). Modulated molecular beam mass spectrometer (MS) was used to monitor the reactants and reaction products in the gas phase.[16-20] Depending on the temperature range, we have used two different flow reactors. The first one (thermostated Pyrex tube, 45 cm length and 2.4 cm i.d.), employed at low temperatures (243 – 320K) has been repeatedly presented previously.[16-20] The inner surface of this reactor as well as of the movable injector of OH were covered with halocarbon wax (HW) in order to reduce the loss of the radicals on the wall. The second reactor, which was recently developed for high temperature kinetic studies (T = 300 - 1000 K), consisted of a Quartz tube (45 cm length and 2.4 cm i.d.) with an electrical heater and water-cooled extremities (Figure 1).[21]
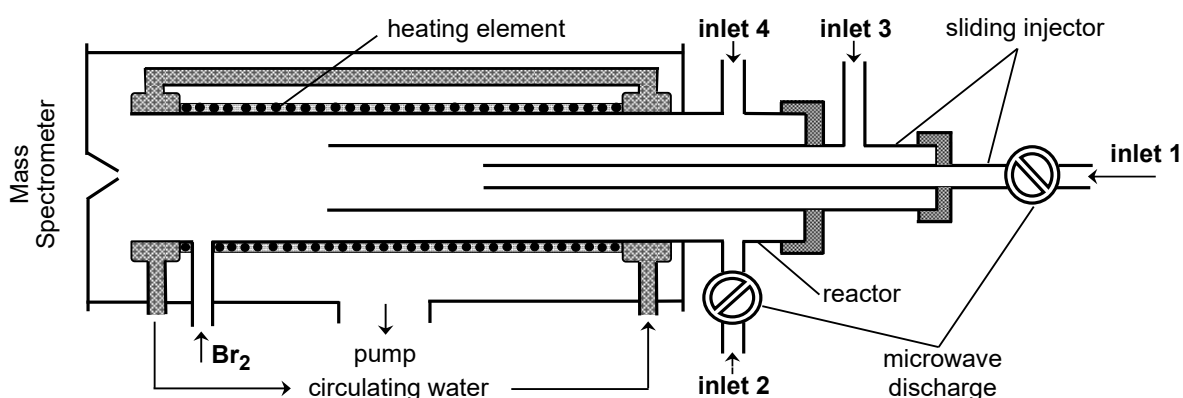
Fig. 1 Diagram of the high-temperature flow reactor.

The inner surface of this reactor was coated with boric acid (BA).[21]

Reaction of H atoms with an excess NO_2 was used to generate OH radicals, hydrogen atoms being produced in a microwave discharge of H_2 diluted with He:

H + NO$_2$ → OH + NO   (2)

Reaction of H atoms with NO$_2$ is known to form vibrationally excited OH radicals. However, under experimental conditions of the present study, the excited OH(v) are rapidly deactivated in reaction with NO$_2$ in the OH-source zone, i.e. before entering the main reactor in contact with p-cymene. Indeed, for residence time in the OH-source zone ≈ 0.005 s, [NO$_2$] = (2-5)×10^{13} molecule cm^{-3} and with rate constant k = 6.4×10^{-11} cm^{3}molecule^{-1}s^{-1} [22] for OH(v) + NO$_2$ relaxation reaction, one can easily calculate that more than 99 % of the vibrationally excited radicals are relaxed to the ground state. In addition, OH(v) can be also deactivated upon collisions with the wall of the movable injector. OH radicals were detected by mass spectrometry as HOBr$^+$ (m/z = 96/98) after being scavenged with an excess of Br$_2$ ([Br$_2$] = (5-10) ×10^{13} molecule cm^{-3}, added 5 cm upstream of the sampling cone) through reaction:

OH + Br$_2$ → HOBr + Br   (3)

The detection of OH with this method was preferable to the direct one at m/z = 17 (OH$^+$), because the traces of water present in the reactor significantly contributed to MS peak at this mass. Reaction (3), quantitatively converting OH to HOBr, was used also for the measurements of the absolute concentrations of OH: [OH] = [HOBr] = Δ[Br$_2$], i.e. concentrations of OH were determined from the consumed fraction of [Br$_2$].[16-17]

The p-cymene vapor was flowed into reactor by passing Helium through a thermostated glass bubbler containing liquid p-cymene (vapor pressure ≈ 2.1 Torr at T = 303 K) or from the calibrated flask (10 L) with known p-cymene/He mixture. In the latter case, the absolute concentration of p-cymene could be calculated from the measured flow rate.

All the relevant species were detected at their parent peaks: m/z= 134 (p-cymene, C$_{10}$H$_{14}^+$), 160 (Br$_2^+$), 96/98 (HOBr$^+$), 88 (1,3-dioxane, C$_4$H$_8$O$_2^+$), 80/82 (HBr$^+$),100 (heptane, C$_7$H$_{16}^+$), 72 (pentane, C$_5$H$_{12}^+$), 46 (NO$_2^+$), 18 (H$_2$O$^+$). The absolute calibrations of MS signals

of the stable species were derived from the measured flows of known mixtures of the species with helium stored in calibrated volume flasks.

The used species and mixtures were: He (>99.9995%, Alphagaz), was passed through liquid nitrogen trap; H_2 (> 99.998%, Alphagaz); Br_2 > (99.99%, Aldrich); HBr (>99.99%, 48% in H_2O, Sigma-Aldrich); NO_2 (> 99%, Alphagaz); n-pentane (> 99.5%, Fluka); n-heptane (> 99%, Sigma-Aldrich); 1,3-dioxane (> 98%, TCI); p-cymene (99%, Aldrich), was degassed before use.

3. RESULTS AND DISCUSSION

3.1. Absolute rate measurements. In these experiments, carried out at nearly 1 Torr total pressure of helium, the rate constant of reaction (1) was determined by monitoring the kinetics of OH consumption in excess of p-cymene. OH radicals were produced in reaction (2), H atoms being flowed into the reactor through inlet 1 (see Figure 1) and NO_2 molecules through inlet 3. P-cymene was introduced through the sidearm of the reactor (inlet 4). The initial concentration of OH radicals was in the range $(3-5)\times10^{11}$ molecule cm^{-3}, the ranges of concentrations of p-cymene at different temperatures are shown in Table 1.

Table 1. Summary of absolute measurements of k_1

T (K)	Reactor Coating[a]	Number/ Kinetics	[P-cymene] (10^{13} molecule cm^{-3})	Stoichiometry ($\Delta[OH]/\Delta[C_{10}H_{14}]$)[b]	k_1 (10^{-11} cm^3 molecule^{-1} s^{-1})[b]
300	HW	7	0.05-0.43	6.33	1.52
320	HW	7	0.12-1.38	2.45	1.22
423	BA	6	0.03-0.20	18.3	0.615
523	BA	5	0.04-0.27	12.5	0.806
603	BA	6	0.05-0.59	4.99	1.09
713	BA	6	0.05-0.62	3.3	1.32
776	BA	10	0.16-2.74	1.15	1.24
898	BA	7	0.24-2.59	1.0	1.53

[a] BA - boric acid, HW - halocarbon wax;
[b] uncertainties on stoichiometric coefficient and on k_1 are nearly 15 and 20%, respectively.

The flow velocity in the reactor was (1600-3790) cm s^{-1}. The concentrations of p-cymene and OH radicals were monitored simultaneously as a function of reaction time. The consumption of p-cymene was found to be insignificant (less than 5%) even when comparable concentrations of OH and p-cymene were used (Table I). As it will be demonstrated below, in these cases consumption of OH was mainly due to the heterogeneous reaction on the wall of the reactor without an associated consumption of p-cymene. Negligible consumption of p-cymene (even at its lowest concentrations used) allows to estimate the possible impact of secondary reactions on the measured OH decays. For the ratio of the rates of OH consumption in primary and secondary gas phase reactions one has: k_1[OH][p-cymene]/k_{sec}[OH][product] > $20 \times k_1/k_{sec}$ (considering that [product] < 0.05×[p-cymene]), i.e. the contribution of secondary chemistry would be limited in most cases, except for the lowest initial [p-cymene] and the longest reaction times, even if the rate constant of secondary reaction, k_{sec}, is up to factor 5 higher than k_1.

Examples of the exponential decays of OH in reaction with p-cymene are presented in Figure 2.
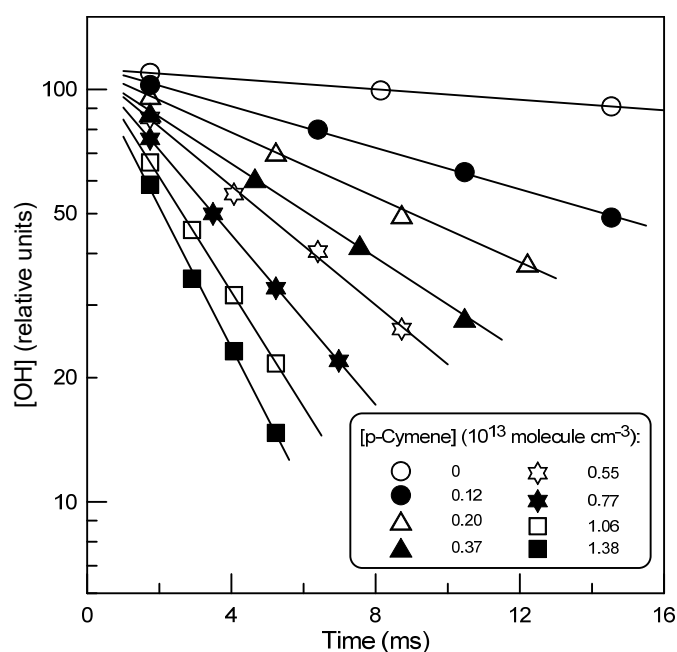
Fig. 2. Example of kinetics of OH consumption in reaction with p-cymene at T = 320 K.

The pseudo-first order rate constant, $k_1' = k_1[\text{p-cymene}] + k_w$, as a function of the concentration of p-cymene is shown in Figure 3. k_w, corresponding to the rate of OH decay in the absence of p-cymene in the reactor, was measured in separate experiments. The pseudo-first-order rate constants were corrected for axial and radial diffusion[23] of OH. The corresponding diffusion coefficient of OH in He was calculated as: $D_0 = 640 \times (T/298)^{1.85}$ Torr cm^2 s^{-1}.[24-26] Applied corrections were mostly less than 10%. The intercepts of the lines in Figure 3 were generally in good agreement with the corresponding values of k_w measured in the absence of p-cymene. The slopes of the straight lines in Figure 3 provide the values of $k_{1\text{measured}}$ at respective temperatures. We intentionally use the term $k_{1\text{measured}}$ instead of k_1 because the measurements of the rate constant of reaction (1) revealed significant contribution of the heterogeneous reaction of OH with surface adsorbed p-cymene practically in the entire temperature range of this study. The impact of the heterogeneous reaction was observed in both reactors (low and high temperature). It was manifested in an anomalous increase of k_1 with decreasing temperature, being stronger in the lower edge of the respective operative temperature ranges.
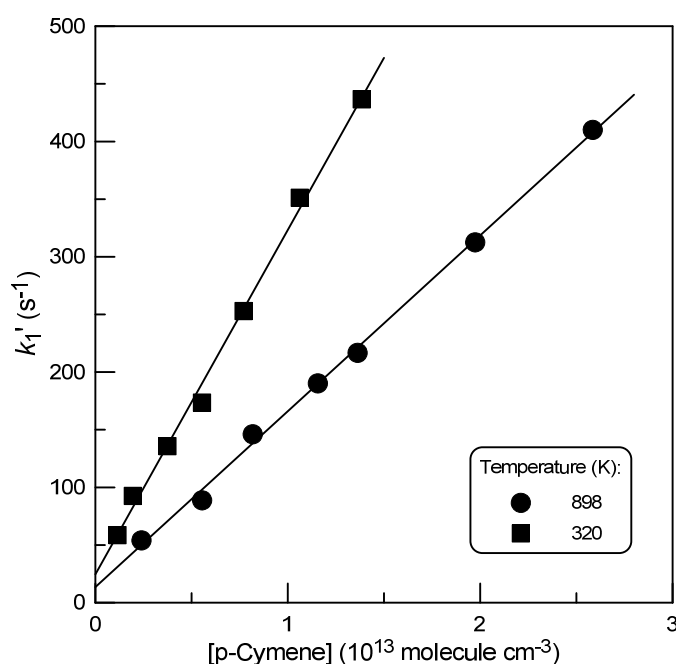
Fig. 3. Pseudo-first order rate constant (k_1') as a function of concentration of p-cymene obtained at T = 320 K and 898 K in reactors coated with halocarbon wax and boric acid, respectively.

To account for the heterogeneous complications and to derive the rate constant of the reaction (1) in the gas phase, we have applied the approach proposed in our recent paper.[21] Based on the experimental observation that dependence of $k_{1measured}$ on concentration of p-cymene is linear (Figure 3, T= 320K), even when contribution of the heterogeneous reaction is very important,

$$d[OH]/dt = -k_{1measured} [OH][p\text{-cymene}] = -\alpha \times k_1 [OH][p\text{-cymene}],$$

and assuming insignificant consumption of p-cymene on the wall of the reactor compared with the consumption of OH, the correction factor α can be identified as the stoichiometry of the reaction, which may be determined experimentally. In that regard, we have carried out additional experiments (for all the temperatures of the study) on determination of the reaction stoichiometry, $\alpha = \Delta[OH]/\Delta[p\text{-cymene}]$, i.e. number of OH radicals lost per one p-cymene molecule. Experiments consisted in a consecutive titration of hydroxyl radicals with an excess Br_2 (to measure $[OH]_0$) and p-cymene accompanied with the measurements of the consumed fraction of these species. Example of the experimental data observed at T = 320 K in the reactor coated with halocarbon wax is shown in Figure 4.
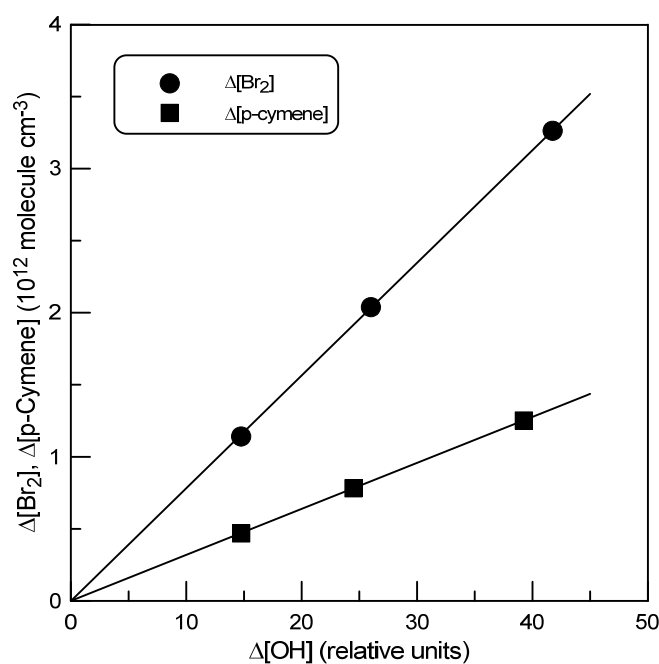
Fig. 4. Consumed fraction of Br_2 and p-cymene as a function of consumed concentration of OH: T = 320 K, reactor coated with halocarbon wax.

The stoichiometric coefficient was determined as a ratio of the slopes of two straight lines in Figure 4 (corresponding to $\Delta[Br_2]$ and Δ[p-cymene], respectively): Δ[OH]/Δ[p-cymene] = 2.45. Dividing by this factor the rate constant resulting from the data in Figure 3 at T = 320 K, $2.99{\times}10^{-11}$ cm^{3}molecule^{-1}s^{-1}, one can obtain the value of k_1 = $1.22{\times}10^{-11}$ cm^{3}molecule^{-1}s^{-1}, corrected for heterogeneous chemistry. This approach was used for determination of k_1 at all temperatures of the study. The correction factors and final values of k_1 are presented in Table 1. As could be expected, the impact of the heterogeneous reaction rises with decreasing temperature. It can be noted that despite impressively high correction factors, the inaccuracy of their measurements, defined by the determination of the consumed fractions of p-cymene and Br_2, was evaluated to be within 15%, leading to nearly 20% combined uncertainty on the measurements of k_1.

It should be emphasized that the employed correction method assumes that p-cymene wall loss is negligible compared with that of OH radical. This condition seems to be satisfied within the present study, and the used correction method seems to be justified, as indicates good agreement of our results with those from earlier studies.[13-14, 27] Nevertheless, for greater confidence in the correctness of the measurements we have conducted additional experiments on the relative rate measurements of k_1 using different reference reactions.

3.2. Relative rate measurements. The relative rate method consisted of the measurements of the consumption of p-cymene and reference compound, simultaneously present in the reactor, in reactions with OH. The relative consumptions of p-cymene and reference compound (Ref) are defined by the rate constants of their reactions with OH:

$$ln\frac{\text{[p-cymene]}_0}{\text{[p-cymene]}} = \frac{k_1}{k_{\text{ref}}} \times ln\frac{\text{[Ref]}_0}{\text{[Ref]}} \qquad (I)$$

where the expressions under the logarithm are the ratios of the compound concentration in the absence of to that in the presence of OH radicals for a given reaction time. The following reactions were used as the reference ones:

$$OH + Br_2 \rightarrow HOBr + Br \qquad (3)$$

$$OH + HBr \rightarrow H_2O + Br \qquad (4)$$

$$OH + 1,3\text{-dioxane} \rightarrow products \qquad (5)$$

$$OH + n\text{-pentane} \rightarrow products \qquad (6)$$

$$OH + n\text{-heptane} \rightarrow products \qquad (7)$$

Experiments were conducted at a total pressure of $(1 - 5)$ Torr of helium. OH radicals were formed directly in the reactor, H atoms being introduced through inlet 2 (Figure 1) and NO_2 molecules through inlet 4. P-cymene and reference compounds were introduced into the reactor through the movable injector (inlets 1 and 3). Initial concentrations of p-cymene and reference compounds were relatively low, $(3 - 8) \times 10^{11}$ molecule cm^{-3}, and that of OH radicals was varied between 5×10^{11} and 5×10^{12} molecule cm^{-3}.
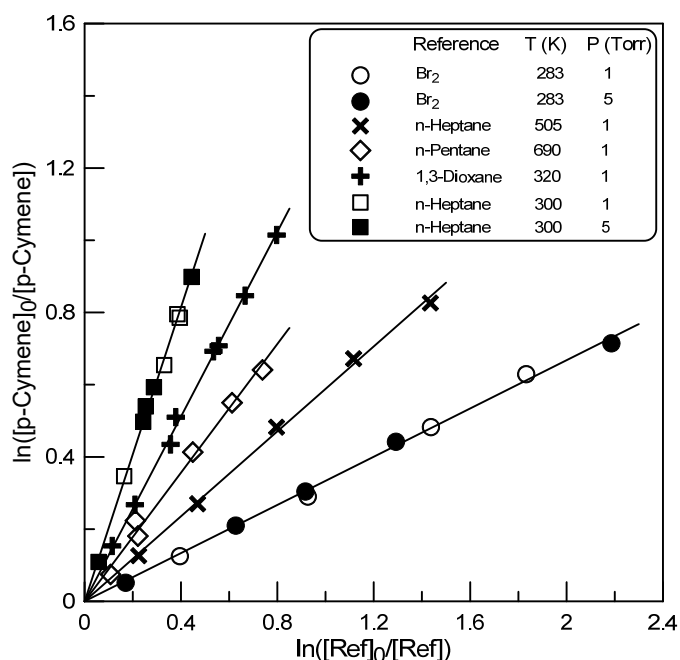
Fig. 5. Examples of $\ln([\text{p-cymene}]_0/[\text{p-cymene}])$ vs $\ln(\text{Ref}]_0/[\text{Ref}])$ dependences observed with different reference compounds and at different temperatures.

Examples of the dependence of $\ln([\text{p-cymene}]_0/[\text{p-cymene}])$ on $\ln([\text{Ref}]_0/[\text{Ref}])$ are shown in Figure 5. According to eq (I) the slopes of the straight lines in Figure 5 represent k_1/k_ref ratio. For the rate constants of the reference reactions we have used the following expressions: $k_3 = 1.96 \times 10^{-9}\ T^{-0.67}$ cm^3 molecule^{-1} s^{-1} at T = 230 – 766,[28] based on three studies of the reaction (3);[17, 28-29] $k_4 = 6.7 \times 10^{-12}$ exp(155/T) cm^3 molecule^{-1} s^{-1}, recommended by Atkinson et al.[30] for T = 180 – 370 K; $k_5 = 6.7 \times 10^{-12}$ exp(121/T) cm^3 molecule^{-1} s^{-1} at T = 253 – 372 K;[31] $k_6 = 9.0\times10^{-17}\ T^{1.8}$ exp(120/T) and $k_7 = 3.75\times10^{-16}\ T^{1.65}$ exp(101/T) cm^3 molecule^{-1} s^{-1} in the temperature ranges (240 - 1300) and (220 – 1300) K, respectively, recommended in a recent study from this group.[21] All the data obtained for k_1 in the relative measurements of the rate constant are presented in Table 2.

Table 2. Summary of the relative rate measurements of k_1.

T (K)	Pressure (Torr)	Number/runs	k_1/k_ref [a]	Reference	k_1 (10^{-11} cm^3 molecule^{-1} s^{-1}) [a]
243	3.0	7	0.471	Br$_2$	2.33
253	1.8	6	1.80	1,3-dioxane	1.95
253	5.0	7	0.417	Br$_2$	2.01
261	1.0	9	1.53	HBr	1.86
262	1.8	6	1.69	1,3-dioxane	1.80
263	5	8	0.396	Br$_2$	1.86
273	1.0	7	1.56	1,3-dioxane	1.63
274	1.0	8	1.43	HBr	1.69
283	1 - 5	9	0.334	Br$_2$	1.49
298	1 - 5	10	0.302	Br$_2$	1.30
298	1.0	5	1.33	HBr	1.50
300	1.0	7	1.38	1,3-dioxane	1.39
300	1-5	9	2.04	n-heptane	1.30
311	5.0	9	0.295	Br$_2$	1.24
320	1.6	8	1.28	1.3-dioxane	1.25
381	1.0	7	0.541	n-heptane	0.480
400	1.0	5	0.950	n-pentane	0.557
426	1.0	5	0.563	n-heptane	0.583

454	1.0	5	0.947	n-pentane	0.673
505	1.0	5	0.587	n-heptane	0.776
548	1.0	6	1.00	n-pentane	0.953
590	1.0	6	0.607	n-heptane	1.01
688	1.0	5	0.598	n-heptane	1.25
690	1.0	6	0.89	n-pentane	1.23

[a] typical uncertainty on k_1/k_{ref} and k_1 is < 5% and nearly 15%, respectively.

3.3. Temperature dependence of k_1. All the data obtained for k_1 in the present work are shown in Figure 6 (filled circles) together with those from previous studies.
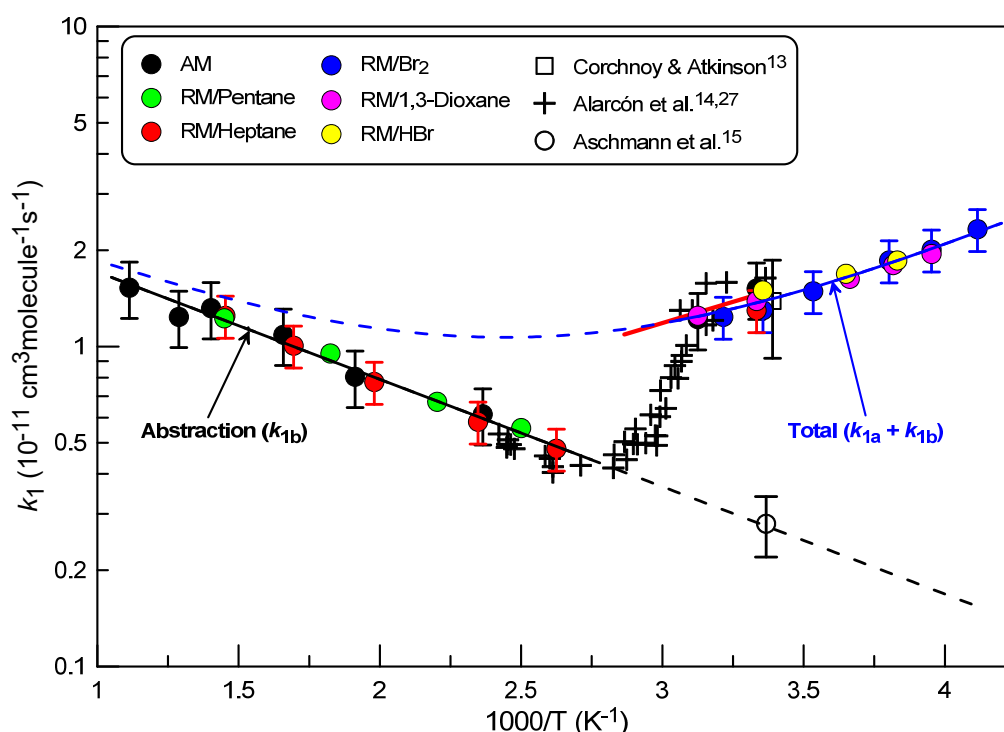
Fig. 6. Summary of the measurements of k_1. For the data from this study: AM, absolute measurements; RM, relative rate method; the error bars correspond to 15 and 20% uncertainties on the relative and absolute measurements of k_1, respectively.

One can note very good agreement between the values of k_1 resulting from the absolute and relative measurements of the rate constant as well as between the relative measurements using different reference reactions. Another point that catches the eye is that our data fully confirm the observations of Alarcon et al.[27] (crosses in Figure 6) who reported a slow decrease of k_1 at T < 320 K, followed by a steeper decrease at T ~ 330K and slow increase at

temperatures higher than 360 K, the latter being attributed to the abstraction channel. In fact, at high temperatures the contribution of the addition channel (1a) to the OH loss is negligible, since the equilibrium

$$OH + C_{10}H_{14} (+M) \leftrightarrows C_{10}H_{14}OH (+M) \qquad\qquad (1a, -1a)$$

is shifted towards the reactants.[14, 27]

We have carried out additional experiments on the detection of the product of reaction (1b), H_2O, in order to obtain experimental evidence of the dominance of the abstraction channel at high temperatures. To avoid the possible impact of the heterogeneous reaction on the distribution of the reaction products, the branching ratio for the H atom abstraction channel of reaction (1) was measured at temperature as high as 810 K where the contribution of the heterogeneous reaction to the consumption of OH was shown to be insignificant (Table I). Experiments consisted in a consecutive titration of the initial concentration of OH with an excess p-cymene and n-heptane accompanied with a direct detection of the reaction product, H_2O. Thereby the yield of H_2O in the reaction of OH with p-cymene was measured relatively to that in the reaction of OH with n-heptane, where the yield of H_2O is 100%. The advantage of this approach is that it does not require absolute calibrations of OH radicals and H_2O.[32] The observed data are shown in Figure 7. The slope of the line in Figure 7 corresponds to the branching ratio for the H atom abstraction channel of reactions (1): 1.00 ± 0.02 (2σ). As one can see from Figure 7 the measured branching ratio is independent of the initial concentration of OH radicals, which was varied in the range: $(0.25 - 1.5) \times 10^{12}$ molecule cm^{-3}. This seems to indicate on the negligible role of the possible formation of water in secondary reactions.
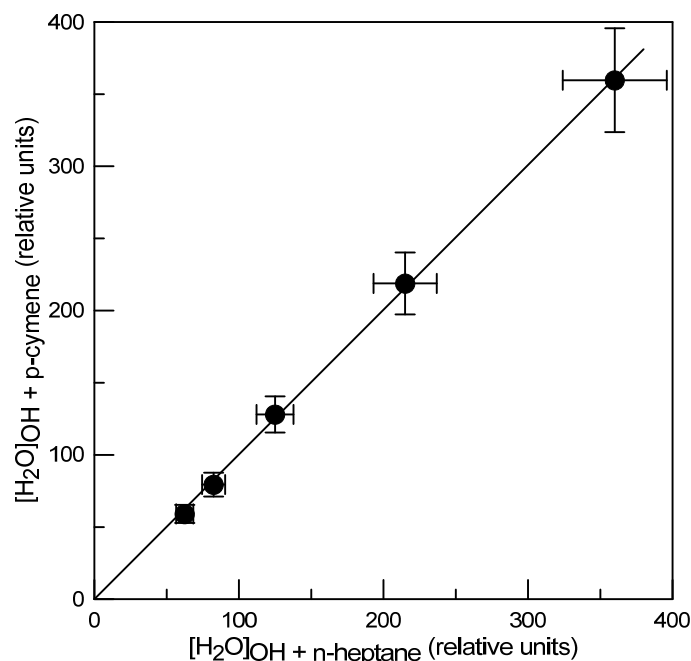
Fig. 7. Concentration of H_2O formed in reaction of OH with p-cymene as a function of the concentration of H_2O formed in reaction of OH with n-heptane upon consumption of the same concentration of OH radicals. Error bars correspond to a maximum uncertainty of 10% on the determination of the relative concentrations.

The unweighted exponential fit to the present data for k_1 at T ≥ 380 K (black solid line in Figure 6), yields the following Arrhenius expression for the rate constant of the abstraction channel of reaction (1) at T = 381 − 898 K:

$$k_{1b} = (3.70 \pm 0.42) \times 10^{-11} \exp(-(772 \pm 72)/T) \text{ cm}^3 \text{ molecule}^{-1} \text{ s}^{-1} \qquad \text{(II),}$$

where the cited uncertainties are 2σ statistical ones. The total rate constant (addition + abstraction) determined by the exponential fit to the present data at T = (243 − 320) K is:

$$k_1 = (1.82 \pm 0.48) \times 10^{-12} \exp((607 \pm 70)/T) \text{ cm}^3 \text{ molecule}^{-1} \text{ s}^{-1} \qquad \text{(III)}$$

Considering the above equation for k_{1b} the total rate constant of reaction (1) can be presented in a biexponential form (blue solid line in Figure 6):

$$k_1 = k_{1a} + k_{1b} = 6.3 \times 10^{-13} \exp(856/T) + 3.7 \times 10^{-11} \exp(-772/T) \text{ cm}^3 \text{ molecule}^{-1} \text{ s}^{-1} \quad \text{(IV)}$$

with nearly 15% conservative uncertainty at T = (243 − 320) K. The dashed blue line on Figure 6 is the extrapolation of this expression to higher temperatures and represents the

hypothetical total rate constant that would be obtained if the collisionally-stabilized adduct would not thermally re-dissociate.

3.4. Comparison with previous studies. The value of k_1 which can be recommended from the present work at T = 298 K is $k_1 = (1.4 \pm 0.2) \times 10^{-11}$ cm^3 molecule^{-1} s^{-1}. This value is in good agreement with previous near room temperature measurements of k_1. Corchnoy and Atkinson[13] using a relative rate method with cyclohexane as a reference compound reported k_1 = $(1.51 \pm 0.41) \times 10^{-11}$ cm^3 molecule^{-1} s^{-1} at T = 295 K. If the rate constant is placed on the absolute basis using $k_{OH + cyclohexane} = 6.90 \times 10^{-12}$ cm^3 molecule^{-1} s^{-1} from more recent evaluation[33] (instead of 7.43×10^{-12} cm^3 molecule^{-1} s^{-1} used by the authors), one gets $k_1 = (1.40 \pm 0.38) \times 10^{-11}$ cm^3 molecule^{-1} s^{-1}. The values reported for k_1 at T = 298 K by Alarcon et al., $(1.57 \pm 0.11) \times 10^{-11}$ [27] and $(1.49 \pm 0.09) \times 10^{-11}$ cm^3 molecule^{-1} s^{-1},[14] are also in agreement with the present data in the range of reported uncertainties.

Alarcon et al.[14] using a reaction model assuming formation of two adducts and resulting in triexponential OH decay curves reanalyzed their previous data (crosses in Figure 6) and extracted the following Arrhenius expression for the sum of OH addition and H-atom abstraction channels of reaction (1): $k_1 = 1.9 \times 10^{-12} \exp((610 \pm 210)/T)$ cm^3 molecule^{-1} s^{-1} between 299 and 349 K (red solid line in Figure 6), which is in excellent agreement with the Arrhenius expression for k_1 obtained in the present study in an extended temperature range (eq III).

It should be noted that the studies of Corchnoy and Atkinson[13] and Alarcon et al.[27] were carried out at a total pressure of 1 atm and (139 - 447) Torr, respectively, while the data from the present study were obtained at nearly 1 Torr pressure. The good agreement between the results obtained at different pressures as well as the independence of k_1 of the pressure in the range (1 − 5) Torr observed in the present study (Figure 5), seems to indicate that the high pressure regime of reaction (1a) extends at least to P = 1 Torr.

Ashmann et al.[15] analyzing the products of the OH + p-cymene reaction in their smog chamber study estimated that H-atom abstraction in reaction (1) accounts for $20 \pm 4\%$ of the overall rate constant at T = 297 K. With $k_1 = 1.40 \times 10^{-11}$ cm^3 molecule^{-1} s^{-1} this leads to the value of $k_{1b} = (0.28 \pm 0.06) \times 10^{-11}$ cm^3 molecule^{-1} s^{-1} (open circle in Figure 6). As one can see on Figure 6, the extrapolation of the expression (II) for k_{1b} obtained in the present study to lower temperatures (black dashed line) is in excellent agreement with this value. Using the expressions for k_{1b} (eq II) and total rate constant k_1 (eq IV) one can estimate the extent of H-atom abstraction channel as a function of temperature: k_{1b}/k_1 increases from 0.2 at room temperature up to 0.7 at T = 500K and 0.9 at T = 900 K.

Regarding the OH addition pathway, Alarcon et al.[14] employing quantum chemical and RRKM calculations showed that OH addition in *ortho* positions to isopropyl and methyl substituents is predominant (55 and 24%, respectively) to those in *ipso* positions (21 and 3%, respectively). The *ipso* adducts formed in reaction (1a) may be subject to dealkylation leading to formation of cresol isomers and alkyl radicals. For example, calculations of Alarcon et al.[14] predicted that more than 90% of the *ipso*-C_3H_7 adduct would react by dealkylation forming p-cresol and isopropyl radicals. On the other hand, Aschmann et al.[15] reported an upper limit of 2% for the formation of cresol from OH + p-cymene system, however, in the presence of oxygen, i.e. under conditions where reaction of adduct with oxygen could compete with dealkylation of adduct. In the present study we have carried out an analysis of the mass spectrum of the products of the reaction OH + p-cymene at T = 298 K. We have observed the appearance of signals at m/z = 151, 136 and 108. The ion peak at m/z = 151 ((CH_3)C_6H_4(C_3H_7)(OH)$^+$) can be attributed to the adduct, p-cymene-OH, which is the main reaction product at room temperature. The signals at m/z = 136 ((OH)C_6H_4(C_3H_7)$^+$) and 108 ((C_3H_7)C_6H_4(OH)$^+$) hypothetically may correspond to p-cuminol and p-cresol, respectively, but most likely are due to fragmentation of the adduct in the ion source of the mass

spectrometer, which was operated at 30 eV energy. In another series of experiments, we have added Br_2 in the reactor (together with p-cymene in the reactor or at the end of the reactor 5 cm upstream of the sampling cone) in order to scavenge the possibly formed alkyl radicals and to transform them into the stable species CH_3Br and $CH_3CHBrCH_3$ via fast reactions (k_8 = 3.88 × 10^{-11} and k_9 = 1.46 × 10^{-10} cm^3 molecule^{-1} s^{-1}):[34]

$$CH_3 + Br_2 \rightarrow CH_3Br + Br \tag{8}$$

$$CH_3CHCH_3 + Br_2 \rightarrow CH_3CHBrCH_3 + Br \tag{9}$$

Indeed, the formation of small however well-defined peaks at m/z = 94 (CH_3Br^+) and 122/124 ($CH_3CHBrCH_3^+$) was observed upon reaction of OH with p-cymene in the presence of Br_2. It should be noted that appearance of these signals does not necessarily indicate on the presence of the corresponding alkyl radicals in the reactive system; they could be due to reactions of Br atoms with p-cymene or Br and Br_2 with p-cymene-OH adduct, followed by the fragmentation of the complex reaction products in the ion source. Taking into account these factors, our data allow to set only the upper limit of 3% (determined as [product]$_{formed}$/[OH]$_{consumed}$) for the formation of either methyl or isopropyl radical in the reaction of OH with p-cymene. However, this upper limit should be treated with caution. The point is that at T = 298 K we have observed significant contribution of the heterogeneous reaction, where the distribution of the reaction products can be different from that in the gas phase reaction. For example, at T = 298 K we have measured the branching ratio of 0.3-0.4 for the abstraction pathway of reaction (1), which is significantly higher than that reported by Aschmann et al.[15] and our extrapolation from high temperature data (nearly 20%). Thereby additional studies are needed to confirm the insignificance of the addition-elimination pathway of the reaction OH + p-cymene.

CONCLUSIONS

In this work, the kinetics and products of the reaction of OH radicals with p-cymene were investigated in the temperature range between 243 and 898 K and at $(1 - 5)$ Torr total pressure. The temperature dependence of the reaction rate constant, measured using both relative rate and absolute methods in an extended temperature range, is in excellent agreement with the previous near room temperature data. The total rate constant (abstraction + addition) as well as the rate constant for H-atom abstraction pathway were determined as function of temperature providing information on the distribution of the reaction products at different temperatures. In particular, the branching ratio for H-atom abstraction channel was estimated to increase from 20% at $T = 298$ to 90% at $T = 900K$. Besides, our results indicate that the reaction route involving OH addition to p-cymene followed by alkyl radical elimination is most probably unimportant.

References

(1) Guenther, A. B.; Jiang, X.; Heald, C. L.; Sakulyanontvittaya, T.; Duhl, T.; Emmons, L. K.; Wang, X. The Model of Emissions of Gases and Aerosols from Nature Version 2.1 (Megan2.1): An Extended and Updated Framework for Modeling Biogenic Emissions. *Geosci. Model Dev.* **2012,** *5*, 1471-1492.

(2) Tsigaridis, K.; Kanakidou, M. Global Modelling of Secondary Organic Aerosol in the Troposphere: A Sensitivity Analysis. *Atm. Chem. Phys.* **2003,** *3*, 1849-1869.

(3) Griffin, R. J.; Cocker, D. R.; Seinfeld, J. H.; Dabdub, D. Estimate of Global Atmospheric Organic Aerosol from Oxidation of Biogenic Hydrocarbons. *Geophys. Res. Lett.* **1999,** *26*, 2721-2724.

(4) Zimmerman, P. R.; Greenberg, J. P.; Westberg, C. E. Measurements of Atmospheric Hydrocarbons and Biogenic Emission Fluxes in the Amazon Boundary-Layer. *J. Geophys. Res. Atmos.* **1988,** *93*, 1407-1416.

(5) Lamb, B.; Guenther, A.; Gay, D.; Westberg, H. A National Inventory of Biogenic Hydrocarbon Emissions. *Atmos. Environ.* **1987,** *21*, 1695-1705.

(6) Papiez, M. R.; Potosnak, M. J.; Goliff, W. S.; Guenther, A. B.; Matsunaga, S. N.; Stockwell, W. R. The Impacts of Reactive Terpene Emissions from Plants on Air Quality in Las Vegas, Nevada. *Atmos. Environ.* **2009,** *43*, 4109-4123.

(7) Henze, D. K.; Seinfeld, J. H. Global Secondary Organic Aerosol from Isoprene Oxidation. *Geophys. Res. Lett.* **2006,** *33*, L09812.

(8) Staudt, M.; Lhoutellier, L. Volatile Organic Compound Emission from Holm Oak Infested by Gypsy Moth Larvae: Evidence for Distinct Responses in Damaged and Undamaged Leaves. *Tree Physiol.* **2007,** *27*, 1433-1440.

(9) Maleknia, S. D.; Vail, T. M.; Cody, R. B.; Sparkman, D. O.; Bell, T. L.; Adams, M. A. Temperature-Dependent Release of Volatile Organic Compounds of Eucalypts by Direct Analysis in Real Time (Dart) Mass Spectrometry. *Rapid Commun. Mass Spectrom.* **2009,** *23*, 2241-2246.

(10) Degenhardt, D.; Lincoln, D. Volatile Emissions from an Odorous Plant in Response to Herbivory and Methyl Jasmonate Exposure. *J Chem Ecol* **2006,** *32*, 725-743.

(11) Gratien, A.; Johnson, S. N.; Ezell, M. J.; Dawson, M. L.; Bennett, R.; Finlayson-Pitts, B. J. Surprising Formation of p-Cymene in the Oxidation of α-Pinene in Air by the Atmospheric Oxidants OH, O_3, and NO_3. *Environ. Sci. Technol.* **2011,** *45*, 2755-2760.

(12) Aschmann, S. M.; Arey, J.; Atkinson, R. Formation of p-Cymene from OH + γ-Terpinene: H-Atom Abstraction from the Cyclohexadiene Ring Structure. *Atmos. Environ.* **2011,** *45*, 4408-4411.

(13) Corchnoy, S. B.; Atkinson, R. Kinetics of the Gas-Phase Reactions of Hydroxyl and Nitrogen Oxide (NO_3) Radicals with 2-Carene, 1,8-Cineole, P-Cymene, and Terpinolene. *Environ. Sci. Technol.* **1990,** *24*, 1497-1502.

(14) Alarcon, P.; Bohn, B.; Zetzsch, C.; Rayez, M.-T.; Rayez, J.-C. Reversible Addition of the OH Radical to p-Cymene in the Gas Phase: Multiple Adduct Formation. Part 2. *Phys. Chem. Chem. Phys.* **2014,** *16*, 17315-17326.

(15) Aschmann, S. M.; Arey, J.; Atkinson, R. Extent of H-Atom Abstraction from OH + p-Cymene and Upper Limits to the Formation of Cresols from OH + m-Xylene and OH + p-Cymene. *Atmos. Environ.* **2010,** *44*, 3970-3975.

(16) Bedjanian, Y.; Le Bras, G.; Poulet, G. Kinetic Study of OH + OH and OD + OD Reactions. *J. Phys. Chem. A* **1999,** *103*, 7017-7025.

(17) Bedjanian, Y.; Le Bras, G.; Poulet, G. Kinetic Study of the Reactions of Br_2 with OH and OD. *Int. J. Chem. Kinet.* **1999,** *31*, 698-704.

(18) Bedjanian, Y.; Riffault, V.; Le Bras, G.; Poulet, G. Kinetic Study of the Reactions of OH and OD with HBr and DBr. *J. Photochem. Photobio. A* **1999,** *128*, 15-25.

(19) Bedjanian, Y.; Riffault, V.; Le Bras, G. Kinetics and Mechanism of the Reaction of OH with ClO. *Int. J. Chem. Kinet.* **2001,** *33*, 587-599.

(20) Bedjanian, Y.; Riffault, V.; Le Bras, G.; Poulet, G. Kinetics and Mechanism of the OH and OD Reactions with BrO. *J. Phys. Chem. A* **2001,** *105*, 6154-6166.

(21) Morin, J.; Romanias, M. N.; Bedjanian, Y. Experimental Study of the Reactions of OH Radicals with Propane, n-Pentane, and n-Heptane over a Wide Temperature Range. *Int. J. Chem. Kinet.* **2015**, *47*, 629-637.

(22) D'Ottone, L.; Bauer, D.; Campuzano-Jost, P.; Fardy, M.; Hynes, A. J. Kinetic and Mechanistic Studies of the Recombination of OH with NO_2: Vibrational Deactivation, Isotopic Scrambling and Product Isomer Branching Ratios. *Faraday Discuss.* **2005**, *130*, 111-123.

(23) Kaufman, F. Kinetics of Elementary Radical Reactions in the Gas Phase. *J. Phys. Chem.* **1984,** *88*, 4909-4917.

(24) Bertram, A. K.; Ivanov, A. V.; Hunter, M.; Molina, L. T.; Molina, M. J. The Reaction Probability of OH on Organic Surfaces of Tropospheric Interest. *J. Phys. Chem. A* **2001,** *105*, 9415 -9421.

(25) Ivanov, A. V.; Trakhtenberg, S.; Bertram, A. K.; Gershenzon, Y. M.; Molina, M. J. OH, HO$_2$, and Ozone Gaseous Diffusion Coefficients. *J. Phys. Chem. A* **2007,** *111*, 1632-1637.

(26) Bedjanian, Y.; Nguyen, M. L.; Le Bras, G. Kinetics of the Reactions of Soot Surface-Bound Polycyclic Aromatic Hydrocarbons with the OH Radicals. *Atmos. Environ.* **2010,** *44*, 1754-1760.

(27) Alarcon, P.; Strekowski, R.; Zetzsch, C. Reversible Addition of the OH Radical to p-Cymene in the Gas Phase: Kinetic Analysis Assuming Formation of a Single Adduct. Part 1. *Phys. Chem. Chem. Phys.* **2013,** *15*, 20105-20114.

(28) Bryukov, M. G.; Dellinger, B.; Knyazev, V. D. Kinetic Study of the Gas-Phase Reaction of OH with Br$_2$. *J. Phys. Chem. A* **2006,** *110*, 9169-9174.

(29) Gilles, M. K.; Burkholder, J. B.; Ravishankara, A. R. Rate Coefficients for the Reaction of OH with Cl$_2$, Br$_2$, and I$_2$ from 235 to 354 K. *Int. J. Chem. Kinet.* **1999,** *31*, 417-424.

(30) Atkinson, R.; Baulch, D. L.; Cox, R. A.; Crowley, J. N.; Hampson, R. F.; Hynes, R. G.; Jenkin, M. E.; Rossi, M. J.; Troe, J. Evaluated Kinetic and Photochemical Data for Atmospheric Chemistry: Volume III - Gas Phase Reactions of Inorganic Halogens. *Atmos. Chem. Phys.* **2007,** *7*, 981-1191.

(31) Moriarty, J.; Sidebottom, H.; Wenger, J.; Mellouki, A.; Le Bras, G. Kinetic Studies on the Reactions of Hydroxyl Radicals with Cyclic Ethers and Aliphatic Diethers. *J. Phys. Chem. A* **2003,** *107*, 1499-1505.

(32) Vandenberk, S.; Peeters, J. The Reaction of Acetaldehyde and Propionaldehyde with Hydroxyl Radicals: Experimental Determination of the Primary H$_2$O Yield at Room Temperature. *J. Photochem. Photobio. A* **2003**, *157*, 269-274.

(33) Atkinson, R. Kinetics of the Gas-Phase Reactions of OH Radicals with Alkanes and Cycloalkanes. *Atmos. Chem. Phys.* **2003,** *3*, 2233-2307.

(34) Timonen, R. S.; Seetula, J. A.; Gutman, D. Kinetics of the Reactions of Alkyl Radicals (CH$_3$, C$_2$H$_5$, *i*-C$_3$H$_7$, and *t*-C$_4$H$_9$) with Molecular Bromine. *J. Phys. Chem.* **1990,** *94*, 3005-3008.

TABLE OF CONTENTS IMAGE